Electron. Mater. Lett., Vol. 12, No. 5 (2016), pp. 568-573
DOI: 10.1007/s13391-016-6075-4

Physical Preparation and Optical Properties of $CuSbS_2$ Nanocrystals by Mechanical Alloying Process

Huihui Zhang, Qishu Xu, and Guolong Tan*

State Key Laboratory of Advanced Technology for Materials Synthesis and Processing, Wuhan University of Technology, Wuhan 430070, China

(received date: 12 March 2016 / accepted date: 10 May 2016 / published date: 10 September 2016)

$CuSbS_2$ nanocrystals have been synthesized through mechanical alloying Cu, Sb and S elemental powders for 40 hs. The optical spectrum of as-milled $CuSbS_2$ nano-powders demonstrates a direct gap of 1.35 eV and an indirect gap of 0.36 eV, which are similar to that of silicon and reveals the evidence for the indirect semiconductor characterization of $CuSbS_2$. Afterwards, $CuSbS_2$ nanocrystals were capped with trioctylphosphine oxide/trioctylphosphine/ pyridine (TOPO/TOP). There appear four sharp absorption peaks within the region of 315 to 355 nm for the dispersion solution containing the capped nanocrystals. The multiple peaks are proposed to be originating from the energy level splitting of 1S electronic state into four discrete sub-levels, where electrons were excited into the conduction band and thus four exciton absorption peaks were produced.

Keywords: $CuSbS_2$, semiconductor nanocrystals, mechanical alloying; optical properties

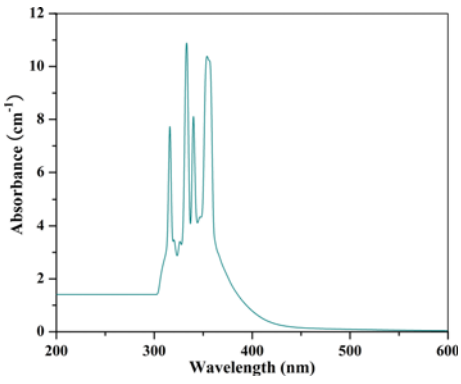

1. INTRODUCTION

As an efficient way to obtain new materials, the alloying of metal chalcogenide nanocrystals (NCs) with different chemical compositions and crystalline structures has attracted intense attention recently, due to their significance in fundamental studies and practical applications.[1-5] Ternary chalcogenides can provide additional degrees of freedom for tuning the electrical and optical properties through chemical composition. With such advantages the ternary semiconductor nanocrystals have been used in both basic research and fields of electric, photoelectric and biological devices.[6-12] It has been reported that $CuSbS_2$ exhibits promising properties, such as a band gap energy of 0.91-1.89 eV and a strong absorption coefficient.[13,14] Although it demonstrates a narrow band gap, it is the best band gap for absorption of solar energy and has the best absorption efficiency.[12-14] Bulk $CuSbS_2$ is comprised of cheap, non-poisonous, readily available, and comparatively abundant elements, making it a sustainable material for semiconductor-based device applications and a particularly attractive candidate for solar photovoltaic.[15]

In recent years, there have been a few reports on the synthesis of $CuSbS_2$ micro and nanocrystals by hydrothermal, solvothermal, and colloidal methods.[16-18] These wet chemical approaches, however, could cause the coverage of organic ligands on surface, and there was some impurity in the fabricated $CuSbS_2$.[19-21] Both factors could somehow screen its intrinsic optical properties. There is thus a need of a complementary synthetic approach which is easily scalable and leads to homogeneous nanocrystals without capping groups.

Mechanical alloying (MA) process is such an approach and has long been demonstrated to be an effective method in promoting mechanochemical reactions at ambient conditions.[22] It has also been shown to be a viable top-down physical approach to generate nanoparticles with sizes smaller than 10 nm.[23-25] This approach is simple and generally run in tens of grams scale and can be easily

*Corresponding author: gltan@whut.edu.cn

scalable. Recently, mechanical alloying (MA) process has been applied to synthesize CdTe,[26] CdSe,[27] CdS[28] nanocrystals and many other types of nanocrystals.[25,29] MA method provides a good pathway to produce surface clean semiconductor nanocrystals, which could be applied to study the intrinsic valence electronic structure and optical excitation behavior of quantum dots, excluding the influence of capping organic ligand on the physical properties of the semiconductor nanocrystals.[30]

Here we report the physical synthesis of surface clean $CuSbS_2$ nanocrystals through MA process. The structure and optical spectrum of the surface clean $CuSbS_2$ nanocrystals will be presented. The capped nanocrystals have average sizes of 4.8 nm, has homogenous size distribution, show an optical spectrum similar to bulk silicon. It could be used as highly promising candidates for solar cell applications replacing silicon.

2. EXPERIMENTAL PROCEDURE

High-purity (99.99%) copper, antimony, and sulfur powders were purchased from Alpha-Aesar. The original weights of each type of elemental powder are 3.8214 g(Cu), 7.3221 g (Sb) and 3.8566 g (S). The raw materials were weighted according to the designed atomic ratio and placed into a stainless steel vial, afterwards four stainless steel balls with various diameters (2-12 mm) were lodged into the vial. The ball to powder mass ratio was set to 10:1. The vial was filled with Ar and sealed in a glove box. The vial was then moved out and mounted on a SPEX 8000M Mixer/mill machine. During different time intervals of the ball milling, small amounts of as-milled powders were taken out from the vial in the glove box for structural and optical measurements. The mechanical alloying process was kept running for 40 hours, after which all as-milled powders were dislodged and stored in a 30 mL glass bottle. The structural evolution of the as-milled powders after different ball milling periods was examined using a Rigaku powder X-ray diffractometer and a JEOL 2100F high-resolution transmission electron microscopy (HRTEM). The optical spectra of the as-milled powders were measured using a Shimadzu UV-3600 spectrophotometer with an ISR3100 integrating sphere attachment. Subsequently, the ball-milled $CuSbS_2$ nanocrystals were capped with trioctylphosphine oxide/trioctylphosphine/pyridine (TOPO/TOP), forming a dispersion solution with yellow color. The optical spectrum and microstructure were also performed upon the dispersion solution of the capped $CuSbS_2$ nanocrystals using the same instruments.

3. RESULTS AND DISCUSSION

3.1 Structural evolution upon mechanical alloying

The X-ray diffraction results show that the initial products of the mechanical alloying process at early stage less than 5 minutes are still Cu, Sb and S elemental powders. Within the first 5 min of the ball milling process, no $CuSbS_2$ were formed, all the diffraction peaks are indexed to the elemental powders. However, when mechanical alloying process was carried out for 10 minutes, $CuSbS_2$ compound was suddenly formed, as being shown in Fig. 1(a), where the diffraction peaks of $CuSbS_2$ compound in orthorhombic structure are observed. At this moment, small trace of diffraction peaks from elemental powders could be still observed at the ball-milling time less than 30 min (Fig. 1(a)-(c)), indicating that a small amount of elemental powders co-existed with the as-milled $CuSbS_2$ compound, in other words, the mechano-chemical reaction of $Cu + Sb + 2S \rightarrow CuSbS_2$ has not been fully completed.

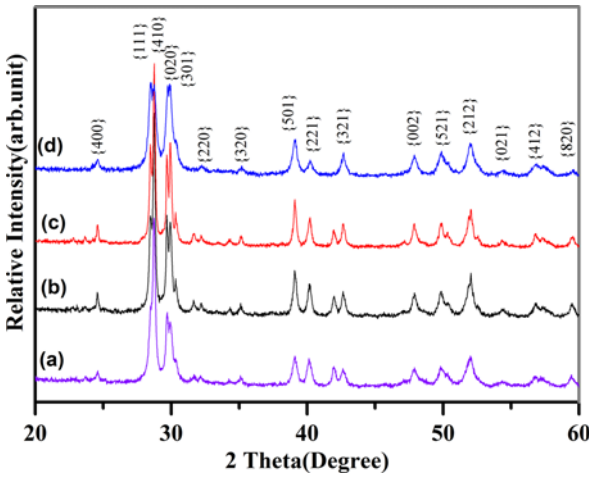

Fig. 1. X-ray diffraction pattern for the products of mechanical alloying elemental Cu, Sb and S powders for (a) 10 min, (b) 15 min, (c) 30 min, (d) 40 h.

When the mechanical alloying process continued further longer, the diffraction peaks from elemental powders became weaker and weaker, until finally they disappeared at the time of 40 hours (Fig. 1(d)). The main diffraction peaks are indexed to the lattice planes of {400}, {111}, {020}, {501}, {321}, {002}, {521} and {212} (Fig. 1(d)), implying the formation of pure $CuSbS_2$ nanocrystals in orthorhombic structure. During the extended ball milling process, there was no change in crystal structure, but the diffraction peaks were broadened and the diffraction intensity was reduced due to the finer grain size. The 40 h as-milled specimens contain a much larger ratio of smaller $CuSbS_2$ nanocrystals, which broadened the diffraction peaks. No second phase or any kinds of impurity were detected after the ball milling process was carried out for 40 hours.

3.2 Microstructure characterization of $CuSbS_2$ nanocrystals

The as-milled $CuSbS_2$ powders exhibit dark colorization

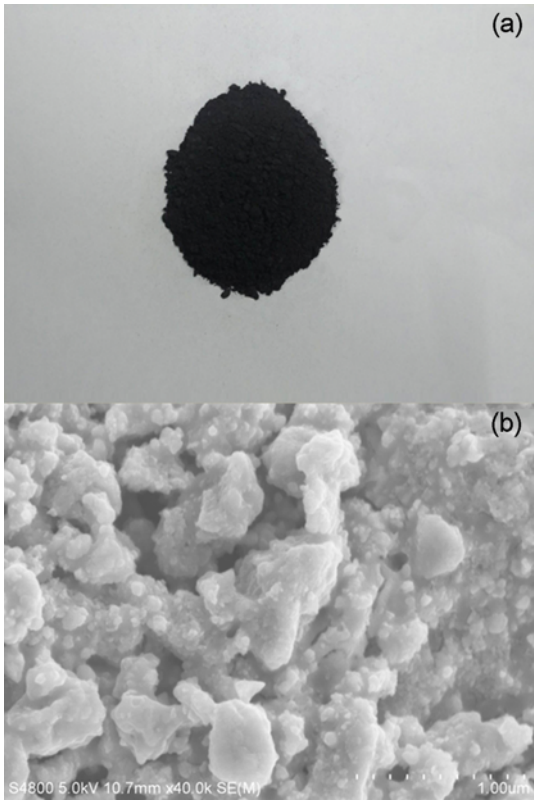

Fig. 2. Photography of piled black specimen (a) and scanning electron microscopy image (SEM) of 40 h as-milled $CuSbS_2$ nanocrystals (b).

after ball milling for 40 hours. Figure 2a shows a pile of the black sample, which was ball-milled for 40 hs and weights around 20 g. Figure 2b displays an image of scanning electron microscopy (SEM) of the as-milled nanoparticles, which demonstrates a certain degree of agglomeration. Small particles aggregate into big particles, some large particles with layered profile are also observed. However, it is difficult to discriminate if such big particles are agglomeration of small individual nanoparticles or only one particle itself due to the limited resolution in the SEM images. Therefore, it is necessary to identify such individual nanoparticles in the transmission electron microscope (TEM) with much higher resolution.

The surface of the as-milled $CuSbS_2$ nanoparticles were then capped with long chain absorption ligand TOPO/TOP. Firstly, TOPO was melted at 55 °C, then 5 mL TOP was poured into the melted TOPO solution to form a mixture of transparent capping solution. Around 0.05 g as-milled $CuSbS_2$ nano-powders was put into a 5 mL glass bottle, into which 2 mL of the TOP/TOPO capping solution was poured. Subsequently, 2.5 mL of pyridine was further added into the bottle, such that a dispersion solution was formed. After several days aging, the dispersion solution containing capped $CuSbS_2$ nanocrystals displayed a yellow color, which

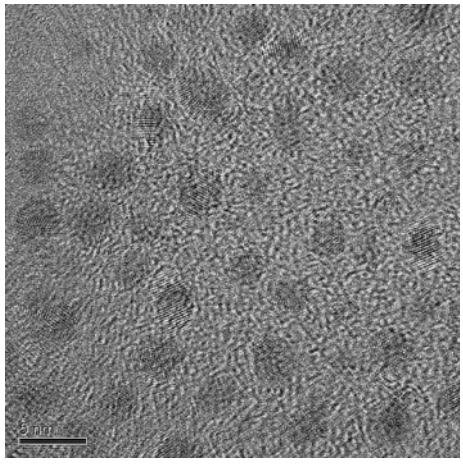

Fig. 3. HRTEM image of the capped $CuSbS_2$ nanocrystals, which were ball milled for 40 h and subsequently capped with TOPO/TOP, then dispersed in pyridine solution.

could keep stable for several months without change. The semi-transparent colorful dispersion solution was stored for optical and TEM measurement. A small amount of dispersion solution was dropped on a holey carbon grid to enable study by transmission electron microscopy.

Figure 3 shows one high resolution transmission electron microscopy (HRTEM) image of capped $CuSbS_2$ nanocrystals in the dispersion solution. Now it is easier to identify those individual nanoparticles in the HRTEM image. It is clearly seen that individual $CuSbS_2$ nanocrystals were homogeneously distributed. Lattice fringes are clearly seen in the image, indicating that the nanocrystals are well crystallized. The lattice fringes of the $CuSbS_2$ nanocrystals are assigned to be {401} and {111} lattice planes (Fig. 3). No aggregation appears for these capped nanocrystals. The long chain molecules on the surface of the $CuSbS_2$ nanocrystals may provide a network to support the $CuSbS_2$ nanocrystals dispersing in the solution, such that the dispersion solution containing the nanocrystals exhibits excellent stability, its color did not change for months.

The statistical results of size distribution for capped $CuSbS_2$ nanocrystals are exhibited in Fig. 4, where the columns represent the statistical count ratio corresponding to the grain size and the fitted line was calculated from the Gauss function. Grain size of the individual nanocrystals was measured upon TEM images of the capped $CuSbS_2$ nanocrystals. Statistical size distribution was calculated from the summarized datum of the individual particle size. It can be seen from Fig. 4 that the grain size ranges from 2.5 nm to 7.5 nm, being centered at 4.7 nm, which could be considered as the average size of the capped $CuSbS_2$ nanocrystals. Figure 4 shows homogeneously size distribution for the capped $CuSbS_2$ nanocrystals, there is no agglomeration after surface capping process.

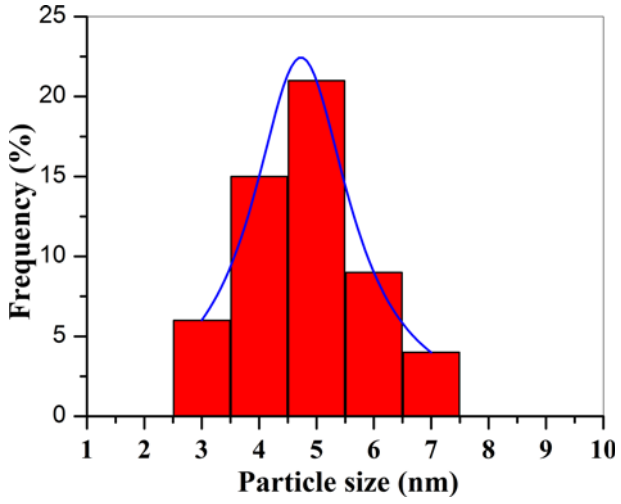

Fig. 4. Statistical size distribution of capped $CuSbS_2$ nanocrystals by TOP/TOPO.

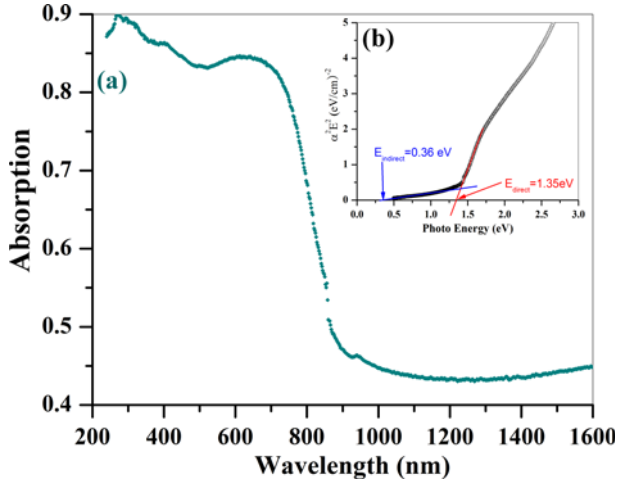

Fig. 5. (a) UV-visible absorption spectra of as-milled $CuSbS_2$ nanocrystals which were ball milled for 40 h; (b) Tauc plot of α^2E^2- as α function of photon energy (E), where a is the absorption coefficient in cm^{-1} and E the photon energy in electron volts (eV).

3.3 Optical properties of $CuSbS_2$ nanocrystals

The reflective spectrum of the 40 h as-milled $CuSbS_2$ nanocrystals were measured using a Shimadzu UV-3600 UV-VIS-NIR spectrophotometer with an ISR3100 integrating sphere attachment, which allows the direct measurement of powder samples. Figure 5 presents a UV-VIS-NIR spectrum of as-milled $CuSbS_2$ nano-powders. The sample has been ball-milled for 40 hs. The as-milled powders were pressed into a round hole (ϕ10 mm) within a sample holder, which was then put into an integral sphere mounted in a UV-3600 spectrometer. The reflectivity of the alloyed nanocrystals was measured through the integral sphere. The reflectivity was then converted to absorbance by Kramers-Kronig transformation.

Figure 5a exhibits the optical spectrum of the as-milled $CuSbS_2$ nanocrystals. It may be seen that a sudden change in absorbance at the wavelength near the band gap energy occurred. The absorbance is very small when the photon energy is less than the band gap energy, since the photons with small energy may not be able to excite the valence electrons to make a transition across the band gap into the conduction band. However, when the photon energy is comparable to the band gap energy, the absorbance demonstrates a sudden increase at the vicinity of the band gap energy (710-950 nm) as being shown in Fig. 5a. The majority of the photons within this energy range were absorbed by the electrons near the top of valence band, those electrons gain the energy from the photons and are then excited to conduction band across the gap, resulting in a sudden rise of the absorbance of the photons. This result reflects the intrinsic valence band structure of as-milled $CuSbS_2$ nanocrystals. The optical spectrum is similar to that of silicon single crystal, but different from that of wet-chemically prepared specimen. These results are also consistent with literature reports and our previous research.[30,38,42] There appears a broad round shaped peak at around 630 nm, which could be contributed to the bounded excitonic absorption. The sharp absorption peak at around 270 nm comes from the electron transition from the inner valence band into the conduction band.

Another transformed spectrum for the plot of α^2E^2 versus E is displayed in Fig. 5b, where α is the absorption coefficient in cm^{-1} and E the photon energy in electron volts (eV). A linear fit to the plot in the region of interest was employed for calculation of the band gap energy of the as-milled $CuSbS_2$ nanocrystals. Linearly extrapolating the α^2E^2 edges with different slope to zero absorption extracts two lines (Fig. 5b). The intersection points of the two extrapolating lines with the X-axis are determined to be direct and indirect band gap energies. The direct and indirect band gap energies are thus estimated to be 1.35 eV and 0.36 eV respectively (Fig. 5b). The direct gap energy is consistent with the reported value in the literatures. It was recognized that copper antimony sulfide ($CuSbS_2$) is a ternary layered semiconductor with a direct band gap between 1.38 and 1.52 eV.[33,35] Ramasamy has synthesized $CuSbS_2$ nanorods and nanoplates through wet chemical method, the optical spectra of these specimens exhibit the characterization of indirect band gap semiconductors, too.[34] The direct and indirect band gap energies of the nanoplates were reported to be 1.4 eV and 1.1 eV respectively. The direct band gap energy of as-milled $CuSbS_2$ nanocrystals is in good agreement with the Ramasamy's value, but the indirect band gap energy is much smaller. The reason for the difference is that the as-milled $CuSbS_2$ has clean surface, while wet-chemically synthesized $CuSbS_2$ nanoplates were capped with long chain organic molecules on the surface.

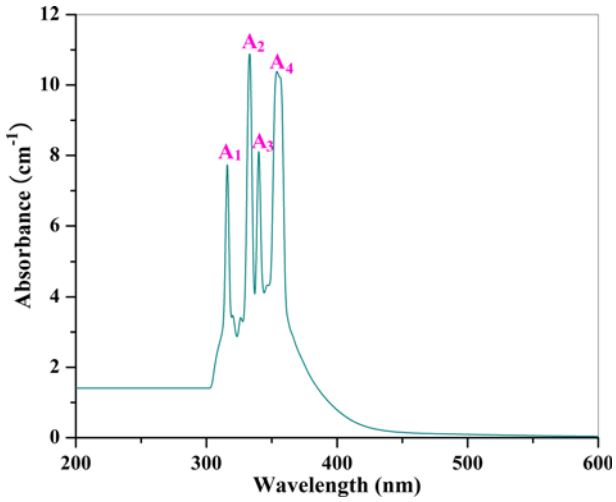

Fig. 6. Optical absorption spectrum of TOP-TOPO capped $CuSbS_2$ nanocrystals, which were ball milled for 40 h and subsequently capped with TOPO/TOP. The capped nanocrystals were then dispersed in pyridine forming a colorful dispersion solution.

The measurement of UV visible optical spectra was performed upon the stable dispersion solution of the capped $CuSbS_2$ nanocrystals. Figure 6 shows the UV visible absorption spectrum of the capped $CuSbS_2$ nanocrystals. The dispersion solution containing capped $CuSbS_2$ nanocrystals exhibits several sharp absorption peaks at 315 nm (A_1), 332 nm (A_2), 340 nm (A_3), and 355 nm (A_4) (Fig. 6). These peaks could be assigned to the bounded excitonic absorbance of capped $CuSbS_2$ nanocrystals. The adjacent multiple sharp peaks result from the spin-orbit splitting of 1S electronic state within the valence band of $CuSbS_2$ nanocrystals. It may be proposed that the 1S electronic state splits into four discrete sub-energy levels, where the electrons originate transition into the conduction band through absorbing the photons with the corresponding energy of the four absorption peaks. The spacing among the discrete sub-energy levels are estimated to be 0.014 eV (A_1-A_2), 0.06 eV (A_2-A_3) and 0.012 eV (A_3-A_4) respectively. The energy level splitting of semiconductor nanocrystals is induced by the quantum confinement effect and was consistent with the observation in CdS nanocrystals.[35] There is a big blue shift of band gap energy in value of around 2.34 eV for capped $CuSbS_2$ nanocrystals in comparison with that of bulk $CuSbS_2$. The reason for the blue shift of band gap energy was also caused by the well known quantum confinement effect when semiconductor particle size is smaller than its Bohr excitation radius.[36] Therefore, both quantum -confinement induced enlargement of band gap and energy level splitting were simultaneously observed in capped $CuSbS_2$ nanocrystals. These results suggest that the as-milled $CuSbS_2$ nanocrystals could also be applied in light emission devices, solar cell and bio-labeling fields after capping process due to their similar optical properties to that of wet-chemically synthesized $CuSbS_2$ nanocrystals.[34]

4. CONCLUSIONS

$CuSbS_2$ nanocrystals have been successfully synthesized by mechanical alloying pure Cu, Sb and S elemental powders under environment condition. The optical spectrum of as-milled $CuSbS_2$ nanocrystals is similar to that of silicon, the direct and indirect bang gap energies are estimated to be 1.35 eV and 0.36 eV, respectively. After capping the surface of as-milled $CuSbS_2$ nanocrystals with TOPO/TOP/pyridine, we obtained a yellow dispersion solution, which shows similar optical properties to that fabricated by a wet chemical method. UV-visible absorption spectra of the capped $CuSbS_2$ nanocrystals exhibit four sharp absorption peaks at 315 nm, 332 nm, 340 nm, and 355 nm. The multiple absorption peaks originates from the quantum confinement effect, which results in energy level splitting of the 1S electronic state into four discrete sub-energy levels. Due to its similar optical spectrum to silicon, $CuSbS_2$ nanocrystals may be also applied for solar cells as sunlight harvest materials replacing silicon.

ACKNOWLEDGEMENTS

The authors acknowledge the financial support from Hubei Natural Science Foundation, under the contract No. 2014CFB166; Open fund of State Key Laboratory of Advanced Technology for Materials Synthesis and Processing (Wuhan University of Technology) under the contract No. 2016-KF-15; as well as the Undergraduate Students' Innovative Foundation of WHUT under the contract No. 20151049701008.

REFERENCES

1. M. V. Kovalenko, M. Scheele, and D. V. Talapin, *Science* **324**, 1417 (2009).
2. S. Li, Z. Zhao, Q. Liu, L. Huang, G. Wang, D. Pan, H. Zhang, and X. He, *Inorg. Chem*. **50**, 11985 (2011).
3. M. D. Regulacio and M. Y. Han, *Acc. Chem. Res*. **43**, 621 (2010).
4. X. G. Peng, *Acc. Chem. Res*. **43**, 1387 (2010).
5. M. A. Malik, M. Afzaal, and P. O'Brien, *Chem. Rev.* **110**, 4417 (2010).
6. K. S. Leschkies, R. Divakar, J. Basu, E. Enache-Pommer, J. E. Boercker, C. B. Carter, U. R. Kortshagen, D. J. Norris, and E. S. Aydil, *Nano Lett*. **7**, 1793 (2007).
7. S. Smith, P. Zhang, T. Gessert, and A. Mascarenhas, *Appl. Phys. Lett*. **85**, 3854 (2004).
8. C. Bertoni, D. Gallardo, S. Dunn, N. Gaponik, and A. Eychmuller, *Appl. Phy. Lett*. **90**, 034107 1 (2007).

9. B. Pukowska, J. Jaglarz, B. Such, T. Wagnerc, A. Kisiela, and A. Mycielski, *J. Alloys Compd*. **335**, 35 (2002).
10. M. Q. Chu, M. X. Song, D. Cheng, S. P. Liu, and J. Zhu, *Nanotechnology* **17**, 5428 (2006).
11. D. Y. Xu, S. L. Shen, Y. J. Zhang, H. W. Gu, and Q. B. Wang, *Inorg. Chem*. **52**, 12958 (2013).
12. M. V. Kovalenko, M. Scheele, and D. V. Talapin, *Science* **324**, 1417 (2009).
13. S. Manolache, A. Duta, L. Isac, M. Nanu, A. Goossens, and A. Schoonma, *Thin Solid Films* **515**, 5957 (2007).
14. B. D. Weil, S. T. Connor, and Y. Cui, *J. Am. Chem. Soc.* **132**, 6642 (2010).
15. J. van Embden, K. Latham, N. W. Duffy, and Y. Tachibana, *J. Am. Chem. Soc*. **135**, 11562 (2013).
16. J. Zhou, G. Q. Bian, Q. Y. Zhu, Y. Zhang, C. Y. Li, and J. Dai, *J. Sol. Stat. Chem.* **182**, 259 (2009).
17. Y. Rodríguez-Lazcano, M. T. S. Nair, and P. K. Nair, *J. Cry. Grow.* **223**, 399 (2001).
18. B. Yang, L. Wang, and J. Han, *Chem. Mater*. **26**, 3135 (2014).
19. Q. Zhang, H. H. Zhang, and G. L. Tan, *Electron. Mater. Lett*. **11**, 187 (2015).
20. R. E. Bailey and S. J. Nie, *J. Am. Chem. Soc*. **125**, 7100 (2003).
21. Y. C. Cao and J. H. Wang, *J. Am. Chem. Soc*. **126**, 14336 (2004).
22. I. J. Lin and S. Nadiv, *Mater. Sci. Eng*. **39**, 193 (1979).
23. P. G. McCormick, T. Tsuzuki, and J. S. Robinson, *J. Ding, Adv. Mater.* **13**, 1008 (2001).
24. Y. Ma, Q. Hao, B. Poudel, Y. C. Lan, B. Yu, D. Z. Wang, G. Chen, and Z. F. Ren, *Nano Lett*. **8**, 2580 (2008).
25. J. L. Guimarães, M. Abbate, S. B. Betim, and M. C. M. Alves, *J. Alloys Compd.* **352**, 16 (2003).
26. G. L. Tan, U. Hommerich, D. Temple, N. Q. Wu, J. G. Zheng, and G. Louts, *Script. Mater*. **48**, 1469 (2003).
27. G. L. Tan, J. H. Du, and Q. J. Zhang, *J. Alloys Compd.* **468**, 421 (2009).
28. G. L. Tan, L. Zhang, and X. F. Yu, *J. Phy. Chem.* C **114**, 290 (2009).
29. P. Balaz, L. Takacs, T. Ohtani, D. E. Mack, E. Boldizarova, V. Soika, and M. Achimovicova, *J. Alloys Compd.* **434-435**, 773 (2007).
30. P. M. Allen, W. H. Liu, V. P. Chauhan, J. Lee, A. Y. Ting, D. Fukumura, R. K. Jain, and M. G. Bawendi, *J. Am. Chem. Soc*. **132**, 2909 (2010).
31. G. L. Tan, S. H. Li, J. B. Murowchick, C. Wisner, N. Leventis, and Z. H. Peng, *J. Appl. Phy.* **110**, 124306 1 (2011).
32. J. T. R. Dufton, A. Walsh, P. M. Panchmatia, L. M. Peter, D. Colombara, and M. S. Islam, *Phy. Chem. Chem. Phy.* **14**, 7229 (2012).
33. C. Yan, Z. Su, E. Gu, T. Cao, J. Yang, J. Liu, F. Liu, Y. Lai, J. Li, and Y. Liu, *J. Mater. Sci. Mater. Electron.* **26**, 1932 (2015).
34. K. Ramasamy, H. Sims, W. H. Butler, and A. Gupta, *J. Am. Chem. Soc*. **136**, 1587 (2014).
35. G. L. Tan, Y. Chen, and X. F. Yu, *Nanotechnology* **21**, 338 (2010).
36. L. Spanhel, M. Haase, H. Weller, and A. Henglein, *J. Am. Chem. Soc*. **109**, 5649 (1987).